International Journal of Scientific & Engineering Research, Volume 5, Issue 10, October-2014
ISSN 2229-5518

Theoretical analysis of distributed reflector laser for low threshold current operation

Syeda Zinath Aman, Nusrat Ferdous, Saeed Mahmud Ullah

Author to whom correspondence should be addressed: E-mail: nferdous07@yahoo.com

Abstract— A large portion of future networks will rely on high speed optical fiber communication systems as fiber-to-the-home (FTTH) which is commercially available at a low cost now a days. For a high-speed large capacity optical fiber network, the functionality of every optical communication equipments should be increased as well as their size should be minimized. Therefore, to increase the functionality of optical communication equipment, it is necessary to improve the performance of individual optical components. This study is mainly focused on analyzing a very low-threshold, high-efficiency and high speed semiconductor laser, which is one of the most important components of the photonic network. In this thesis, distributed reflector (DR) lasers, consisting of a DFB (distributed feedback) laser with high reflection DBR (distributed Bragg reflectors) on one end, is studied by considering wire-like active regions for the DFB section. Performance of the DR lasers with quantum wire structures has been analyzed here on the basis of dependence of threshold currents on Facet Phase, effect of Phase Shift, and on the number of Quantum Wells (QW) present in the laser structure. The theoretical results observed ensure high potential of DR laser for very low threshold current operation with high efficiency.

Index Terms: Distributed feedback laser, Distributed Reflector, Facet Phase, Optical Fiber Network, Phase Shift, Quantum Well, Threshold Current.

1. Introduction

As the optical fiber communication systems are widely spread throughout the society, the development of communication equipment for a high-speed large-capacity optical fiber network is required. To increase the functionality of optical communication equipment, it is necessary not only to improve the performance of individual optical components, but also to increase the number of mounted components. However, in order that information can be carried along the Single Mode Fiber (SMF), information at the transmitter side is first converted into a stream of coherent photons. Using a specially designed semiconductor junction diode with heavy doping concentration, semiconductor lasers have been used to provide the reliable optical source required in fiber based light wave communication. With its miniature size compatible to the SMF, the semiconductor lasers have played a crucial role in the success of optical fiber communication systems [1].

The semiconductor laser oscillating with ultra low threshold current is a key device for high-density parallel optical interconnections. The turn-on delay-time depends on the threshold current of the laser because of a limited carrier lifetime in the active layer. Therefore, a skew problem between the channels of a parallel transmission system can be reduced by decreasing the threshold current.

When the differential quantum efficiency of the laser is kept at 0.3 W/A, the lowest threshold current, which still yields a drive power advantage, is approximately 100 μA for 100 Mb/s, 50 μA for 1Gb/s, and 10 μA for 5 Gb/s data rate. Shin et al discussed the electrical power advantage as a function of the threshold current for error free (bit error rate: BER < 10-9) data communications when the differential quantum efficiency of the ultra-low threshold current laser is changed by the cavity length and the facet reflectivity [2].
A threshold current of semiconductor lasers can be written as:

$$I_{th} = eB_{eff}V_a[N_g + \frac{1}{\xi g'}(\alpha_{wg} + \alpha_m)]^2$$

where e is the electron charge, V_a is the active medium volume, B_{eff} is the effective spontaneous recombination coefficient, N_g is the transparent carrier density, ξ is the optical confinement factor, $g' = \frac{\partial g}{\partial N}$ is the differential gain, α_{WG} is the waveguide loss and α_m is the mirror loss, respectively. Low threshold current operations can be realized by small V_a, large ξ, large g′ and small α_m.

Syeda Zinath Aman, Assistant Professor, Department of Electronics and Communication Engineering, Institute of Science and Technology, Dhaka, Bangladesh. E-mail: ami.apece@gmail.com
Nusrat Ferdous , Lecturer, Department of Electronics and Communication Engineering, Institute of Science and Technology, Dhaka, Bangladesh. E-mail: nferdous07@yahoo.com
Saeed Mahmud Ullah,Assistant Professor, Department of Applied Physics, Electronics and Communication Engineering, University of Dhaka, Bangladesh. E-mail: ullahsm@du.ac.bd

In order to realize the low threshold current operation, several laser structures have been reported. Vertical-cavity surface emitting lasers (VCSELs), short cavity edge emitting lasers with high-reflection (HR) coatings or distributed Bragg reflectors (DBRs) and micro disk lasers can be operated at the low threshold current due to their small active medium volume with high-reflectivity mirrors. Distributed Feedback (DFB) lasers have been developed for optical fiber communications as dynamic single-mode (DSM) lasers [3]. In a very early stage in the development of optical fiber communication systems, transmitters were multimode lasers. However, using multimode lasers, transmission speed and distance are limited by dispersion in optical fibers. DSM lasers would enable transmission over long distances at high bit rates. Recently, DFB laser arrays for WDM systems have been reported [4,5].

Moreover, for high efficiency operation, distributed reflector (DR) lasers which consist of a DFB and a DBR sections have been investigated and it was found that they have superior dynamic properties such as modulation sensitivity and spectral chirping [6]. In addition, DR lasers with the vertical grating (VG) were demonstrated to have high-efficiency and single-mode operation due to their high-reflection DBR by deep etching technology [7].

In this work, width-modulated structures of DR lasers have been studied to find out the optimum conditions to have highly efficient DR lasers which work with very low threshold current.

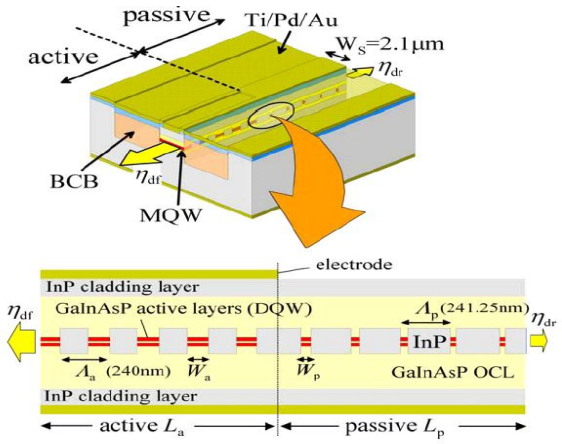

Fig. 1 Schematic diagram of Distributed Reflector (DR) laser and its cross sectional side view.

1. Distributed Reflector (DR) Laser

Distributed Reflector laser or DR laser is the first example of integrated device fabricated using wire-width modulated active regions utilizing lateral quantum confinement effect. Fig. 1 shows the schematic diagram of the DR laser. The side view of the schematic diagram shows a DR laser consisting of an active DFB section with wirelike active regions and a passive grating section at the right side with quantum-wire (Q-wire) structure where La, Λa,Wa, Lp, Λp and Wp denote the section length, the grating period, the width, in the active section and the section length, the grating period, the width, in the passive section, respectively. These sections were integrated by utilizing the lateral quantum confinement effect by modulating the wire-like active regions. The passive DBR section acts as a highly reflective DBR in order to concentrate the output power onto only one facet, which leads to an increase in the output efficiency while maintaining a low-threshold current. For high performance operation, that is low-threshold and high-efficiency operation, DBR reflectivity should be as high as possible. In order to realize the DBR with high reflectivity, it is necessary to reduce the waveguide loss. For this purpose, extension of the transition energy, which is called "blue shift", due to the lateral quantum confinement effect by using the Q-wire structure for the DBR section is applied [1]. The transition energy in the passive section is expected to be much larger than that in the active section. Therefore, the active and passive sections can be integrated by adopting width-modulated active regions. The integration technique utilizing the energy blue shift is reported to be advantageous regarding low-loss coupling, the short transition length between two sections and good crystal quality.

2.1 Characteristics of DBR passive section with quantum wire structure

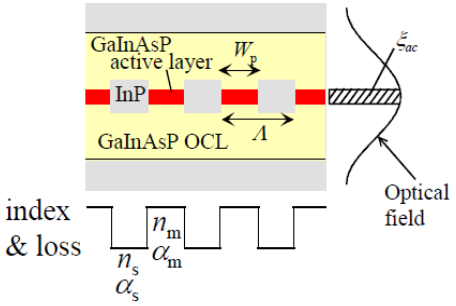

Fig. 2.1 DR structure

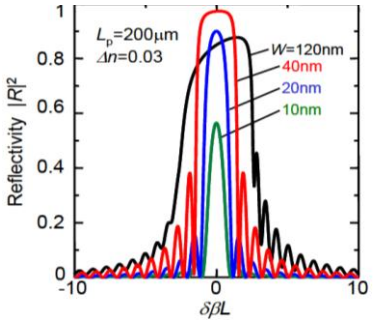

Fig. 2.2 Reflectivity dependence on DBR section wire-width[8]

The schematic structure of DR section is shown in Fig. 2.1. The grating period and wire width are denoted by Λ=240 nm and w_p, respectively. The propagation loss in the active and passive external layers and optical confinement factor are listed in Table 2.1. Fig. 2.2 shows results of the DBR reflectivity dependence on DBR section length[8]. Assuming facet reflectivity be 30%, this calculation was performed using the transfer matrix method (TMM)[8]. Results for w_p of 10, 20, 40 and 120 nm are shown, where the absorption loss for each wire width was taken into consideration. The refractive index difference Δn of 0.03, a grating pitch Λp of 240 nm and a double quantum well (DQW) structure were assumed.

Λ	240 nm
α_{ac}	100 cm^{-1}
α_{ex}	4 cm^{-1}
ξ_t	1%/layer

Table 2.1. Parameters for calculation

2.2 Facet phase of DR Laser

In DR laser with wire-like grating structure, the effect of facet phase is one of the main concerns. A schematic diagram of the corrugation pattern and the relation of the facet phase and the position of the cleaved facet have been shown in Fig. 2.3. Since DR laser usually has cleaved front facet, it plays a role in static characteristics. Moreover, due to manual cleaving it is not possible to predict the condition of the facet. However, the influence of facet phase condition can be nullified by applying anti reflection (AR) coating. In the offset of Fig. 2.3, we have defined the phase of the facet depending on grating position. The facet phase will be denoted by φ from now on. φ =0 is considered if facet ends at the middle of the gain region of the grating. At the falling end of the grating is φ =π/2. At the middle of the non-gain region, φ = π. φ = 3π/2 assumed at the rising end the grating.

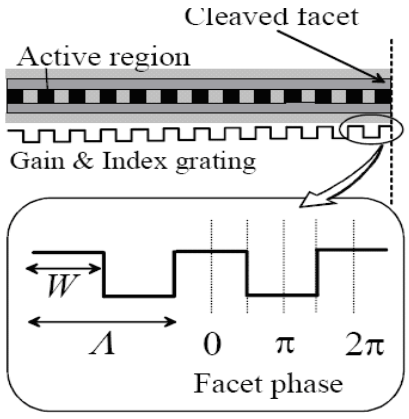

Fig. 2.3 Definition of the front facet of the DFB Section

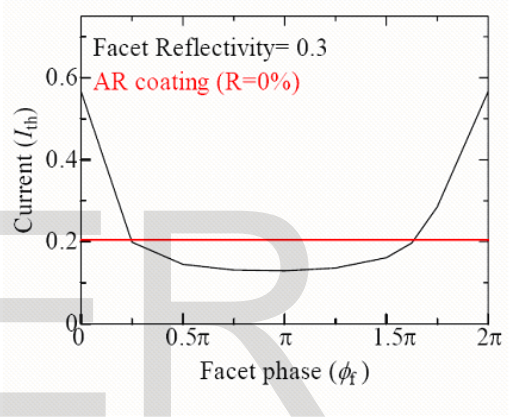

Fig. 2.4 Threshold current for different facet phase.

Fig. 2.4 shows the Threshold current for different facet phase. Fig. 2.4 shows the threshold current dependency on the facet phase reported [2]. The DFB section length has been considered to be 200 μm. As the cleaving facet moves away from the middle of the upper grating (Fig. 2.3), the cancellation of anti-phase reflection at the facet is reduced and thereby residual reflection increases and consequently threshold current is decreased.

3. Analysis of DR Laser for Low threshold Current Operation

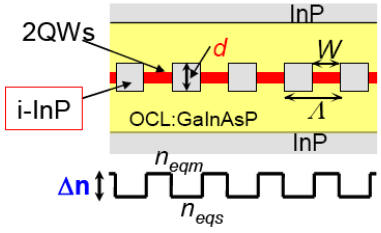

Fig. 3.1 Refractive index profile of DFB cavity

Fig. 3.1 shows the refractive index profile of the active region where the equivalent refractive indices of gain and non-gain regions are denoted as n_{eqm} and n_{eqs} , respectively. The difference of these two equivalent refractive indices has been denoted as Δn as mentioned earlier. For a wire-like DFB region with a wire width ratio (Wa/ Λa) of 0.5 and Δn=0.03.

In this work, it is theoretically analyzed to achieve lower threshold current under different conditions using C programming. Providing different conditions, several graphs have been obtained, which reveals dependence of threshold current on different parameters. The respective graphs are discussed below.

4. Dependence of threshold current of DR Laser

4.1 Number of Quantum Well

In our study, we have found that, for single Quantum Well (QW), threshold current was very high till the Cavity Length (CL) of 149.75 μm, after that level it came down and reached the lowest level of 0.17mA and it remained constant from 230 μm to 339 μm.

For the 2nd QW, I_{th} was very high till the CL of 80 μm. After that it declined till 249μm CL. But at the last level it increased up to 0.21mA.

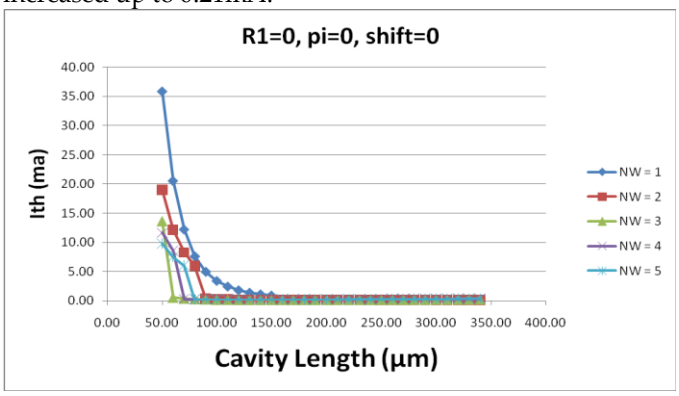

Fig. 4.1 Dependence of Threshold Current on QW number.

In case of 3rd QW, the threshold current value was gradually declining till the CL of 179 μm and afterwards it started to go up and touched the level of 0.26mA.

Similar to the 3rd QW, the 4th also had a 2 stage movement of the values. It also declined up to the CL of 159 μm and then started to increase up to 0.31mA.

The 5th QW gave the highest value among the five options. It lastly reached the value of 0.37mA.

Finally this is observed from the Fig. 4.1, that the lowest value of the threshold current 0.16mA was achieved for the 2QW lasers at the CL of 200 μm.

4.2 Facet phase reflections

In DR laser with wire-like grating structure, the effect of facet phase is one of the main concerns. A schematic diagram of the corrugation pattern and the relation of the facet phase and the position of the cleaved facet have been shown in Fig. 2.3. Since DR laser usually has cleaved front facet, it plays a role in static characteristics. Moreover, due to manual cleaving it is not possible to predict the condition of the facet. However, the influence of facet phase condition can be nullified by applying anti reflection (AR) coating. In the offset of Fig. 2.3, the phase of the facet is defined depending on grating position. The facet phase will be denoted by ϕ from now on. ϕ =0 is considered if facet ends at the middle of the gain region of the grating. At the falling end of the grating is ϕ =π/2. At the middle of the non-gain region, ϕ = π. Φ = 3π/2 assumed at the rising end the grating.

The reduction of a threshold current after AR coating can be attributed to the facet phase effect. It is observed that after AR coating values for various facet phases remain almost same for both single and double QW.

We got that, for the single QW, the lowest threshold current 0.17mA is achieved at the CL of 230μm and remained constant afterwards.

On the other hand, in case of double QW, the lowest threshold current 0.16mA is achieved at the CL of 200 μm and after that level it started to increase and reached up to the level of 0.2mA.

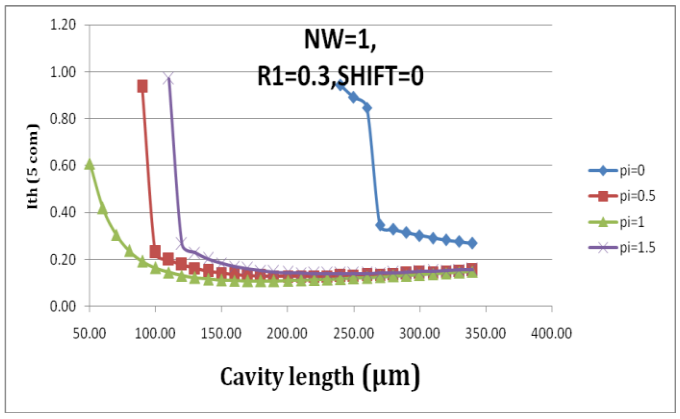

Fig. 4.2 Facet phase dependence of threshold current for single quantum well and Reflectivity = 0.3

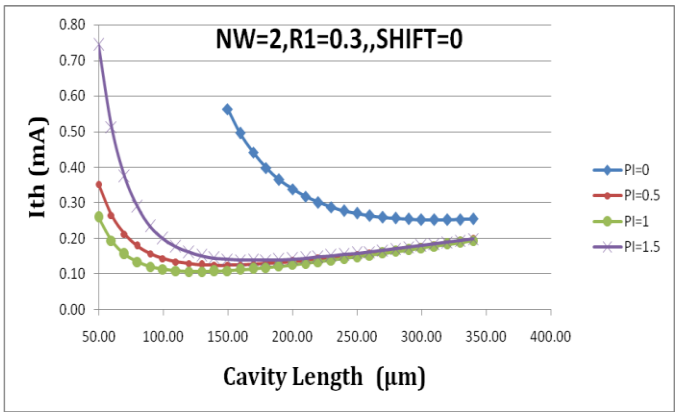

Fig. 4.3 Facet phase dependence of threshold current for double quantum well and Reflectivity = 0.3

Fig. 4.2 shows the effects of facet phase shifts for single quantum well. Four different phases were analyzed. This is observed that the 1st phase where $\pi = 0$, gives higher value from the very beginning. That means the 1st phase provides higher results at the CL of 50 – 259 μm. After that it declined and ended at 0.27mA.

The second phase, with $\pi = 0.5$, started at a higher value but at the middle it declined to 0.13mA and ended at 0.16mA.

The 3rd one where $\pi = 1.0$, provided the best result among these four phases. It gave 0.11mA at the level of 149μm that was quite well.

Finally phase with $\pi = 1.5$, though started with an abnormal figure, it declined gradually later, but the results were not so close to the best.

Fig. 4.3 shows the effects of facet phase shifts for double quantum well. Four different phases were analyzed in this case also. This is observed that the 1st phase where $\pi = 0$, gives higher value from the very beginning. That means the 1st phase provides higher results at the CL of 50 – 139 μm. After that it declined and ended at 0.25mA at CL of 339 μm.

The second phase, with $\pi = 0.5$, started from 0.35mA then it gradually declined to 0.12 at the CL of 139μm. After that it again increased and ended at 0.20mA at CL of 339μm.

The 3rd one, where $\pi = 1.0$ provided the best result among these four phases. It started with lower value of 0.26mA which is lower than that of the second phase. It reached 0.11 for the CL of 99-169 μm after that it started to go upward and ended at 0.19mA at CL of 339 μm.

The 4th phase, where $\pi = 1.5$, the current started with 0.76mA. It reached 0.14mA for the CL of 139-210μm, after that it started to go upward and ended at 0.20mA for CL of 339μm.

From the observations the best result is found to be 0.11mA, which was found at the 3rd phase with $\pi = 1.0$ at the CL of 99 μm.

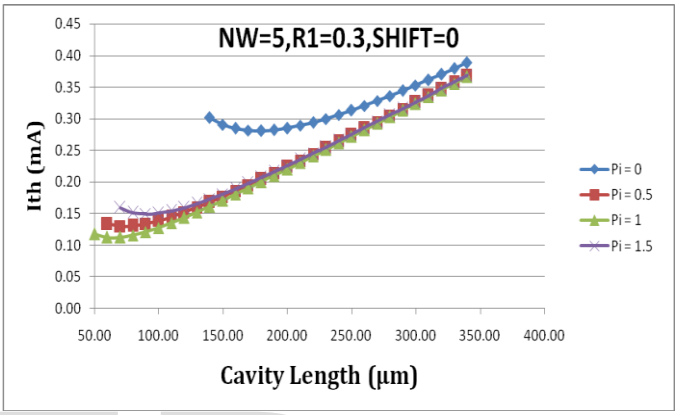

Fig. 4.4 Facet phase dependence of threshold current for five quantum well and Reflectivity = 0.3

In Fig. 4.4, four different phases were analyzed for five quantum well. This is observed that the 1st phase, where $\pi = 0$, gives higher value ranging from 2.77mA - 0.39mA. At the middle stage, it declined to 0.28mA for the CL of 159 μm and after 189 μm it started to go up.

The second phase, with $\pi = 0.5$, started with 0.13mA, then it gradually increased and ended at 0.37mA for CL of 339 μm.

In case of the 3rd one, where $\pi = 1.0$, it started with lower value of 0.12mA. Then it declined to 0.11mA for the next two CL. After that it started to go up and ended at 0.37mA for CL of 339μm.

The 4th phase, where $\pi = 1.5$. It started with 0.16mA. It reached 0.15mA for the CL of 80-109μm after that it started to go upward and ended at 0.37mA for CL of 339 μm.

From the observations the best result is found to be 0.11mA which was found at the 3rd phase with $\pi = 1.0$ at the CL of 60 μm.

4.3 Effects of phase shift

An effect of phase shift inserted in DFB lasers with wire-like active regions is analyzed. Initially, $\lambda/4$ phase shifted DFB lasers were developed in order to realize a highly reliable dynamic single mode (DSM) laser, in which the main longitudinal mode could be obtained at the center of the stop-band, i.e., the Bragg wavelength. Since the resonant mode at the Bragg wavelength undergoes the strongest feedback and has the lowest required threshold gain, therefore, the phase shift is also effective in the low threshold current operation.

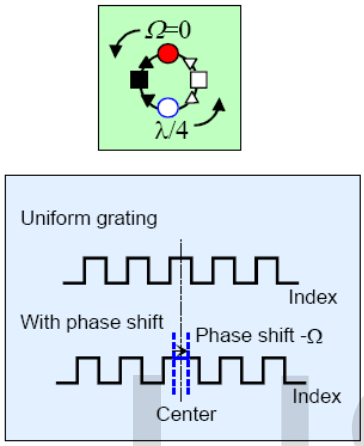

Fig. 4.5 Phase Shift dependence of threshold current

Lasing modes are dependent on phase shift value. By introducing the phase shift, the lasing mode generates into the stop-band in the case of uniform grating. In the case of $\lambda/4$ phase shift, the lasing mode is the Bragg wavelength, (while it is actually a little bit shorter than the Bragg wavelength due to the gain coupling.)

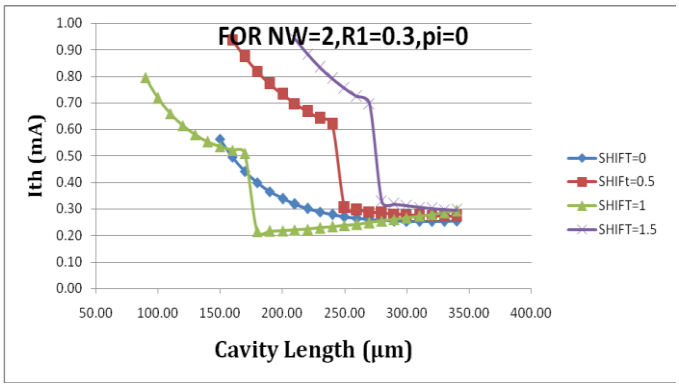

Fig. 4.6 Effect of phase shift on threshold current for double QW

Fig. 4.6 shows the effects of the phase shift on threshold current for double quantum well. Here, four different shifts were taken under consideration. In case of shift = 0, the results began with higher values for the CL of 50-139 μm and then declined to 0.35mA at the CL of 339 μm.
When shift = 0.5, the results began with higher values for the CL of 50-240 μm and then declined to 0.27mA for the CL of 339μm.

In case of shift = 1.0 the results began with higher values for the CL of 50-169 μm and then declined to 0.29mA for the CL of 339μm.

In the last case, when shift = 1.50 then the results began with higher values for the CL of 50-269 μm and then declined to 0.30mA for the CL of 339 μm.

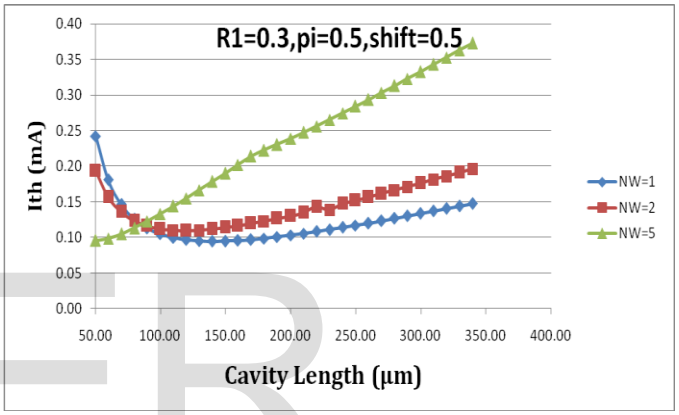

Fig. 4.7 Comparison among QWs forR1 = 0.3, π = 0.5, shift = 0.5

In Fig. 4.7, in case of single QW the results started with a lower value of 0.24mA and declined till 149μm. In this range, the lowest value achieved was 0.09mA. After that, it started to move upward and ended at 0.15mA for the CL of 339 μm

For the double QW the results started with 0.19mA and declined to 0.11mA for the CL of 149μm. After that it gradually increased and ended at 0.20mA for the CL of 339μm.
For the 5QW the results began at the lowest value of 0.10mA and continued to increase and at last ended at 0.37mA for the CL of 339 μm.

Comparing these three scenarios, this is observed that the best result is achieved for single QW which is 0.09mA at the CL of 139μm. But in terms of CL the best result is provided by 5QW where threshold current of 0.10mA is achieved for the CL of 50 μm.

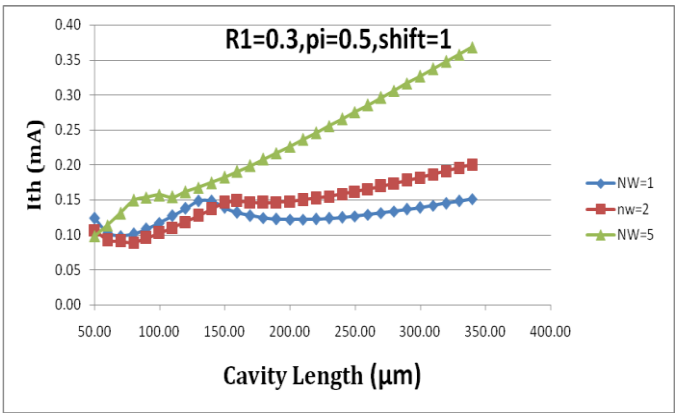

Fig. 4.8 Comparison among QWs forR1 = 0.3, π = 0.5, shift = 1

In Fig. 4.8, in case of single QW the results started with a lower value of 0.12mA after that the values were very fluctuating they increased and decreased several times. At first it gradually declined to 0.10mA till the CL of 80 μm. After that it increased up to 139μm. Then again it started to fall till the CL of 240μm and reached 0.12mA. It further increased and ended at 0.15mA at CL of 339μm.

For the double QW the results started with 0.11mA and declined to 0.09mA for the CL of 60 μm. After that it gradually increased and ended at 0.20 for the CL of 339 μm.

For the 5QW the results were almost same as that for the shift = 0.5 in Fig. 4.6. Just a simple difference is that the value at the CL of 109 μm had a little decline.

Comparing these three scenarios this is observed that the best result is achieved both in terms of CL and Threshold Current for double QW which is 0.09mA for the CL of 60 μm.

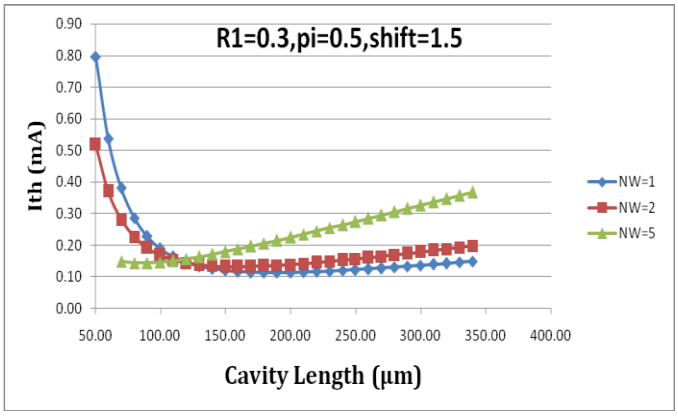

Fig. 4.9 Comparison among QWs forR1 = 0.3, π = 0.5, shift = 1.5

In Fig. 4.9, in case of single QW the results started with a lower value of 0.80mA after that the values gradually declined to 0.11mA till the CL of 200μm. It further increased and ended at 0.15mA for CL of 339 μm.

For the double QW the results started with 0.52mA and declined to 0.13mA for the CL of 139 μm. After that it gradually increased and ended at 0.20 for the CL of 339 μm.

For the 5QW the results started with 0.15 for the CL of 70 μm and then it gradually increased to end at 0.37 for the CL of 339 μm.
Comparing these three scenarios this is observed that the best result is achieved for Single QW which is 0.11mA for the CL of 169 μm.

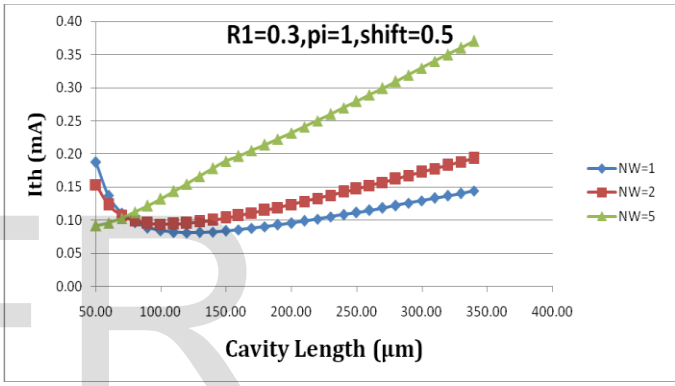

Fig. 4.10 Comparison among QWs forR1 = 0.3, π = 1, shift = 0.5

In Fig. 4.10, in case of single QW the results started with a lower value of 0.19mA after that the values gradually declined to 0.08mA till the CL of 100μm. It remained same until 149μm. It further increased and ended at 0.14mA at CL of 339 μm.

For the double QW the results started with 0.15mA and declined to 0.09mA for the CL of 109μm. After that it gradually increased and ended at 0.19 for the CL of 339 μm.

For the 5QW the results started with a lower value of 0.09mA for the CL of 50μm and then it gradually increased to end at 0.37 for the CL of 339μm.

Comparing these three scenarios this is observed that the best result is achieved for Single QW in terms of threshold
Comparing these three scenarios this is observed that the best result is achieved for Single QW in terms of threshold

current which is 0.08mA for the CL of 99 μm and in terms of CL the best result is provided by the 5QW that provided threshold current 0.09mA for the CL of 50 μm.

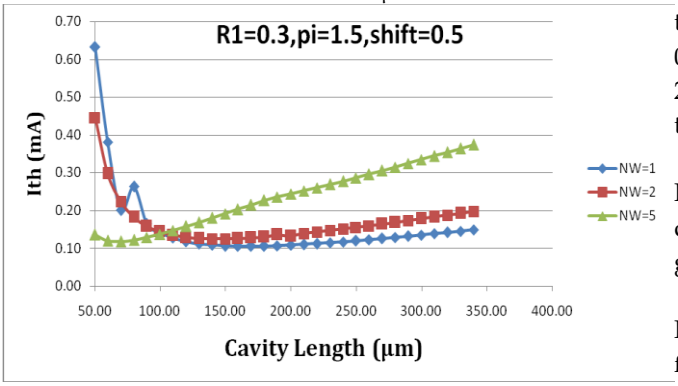

Fig: 4.11 Comparison among QWs forR1 = 0.3, π = 1.5, shift = 0.5

In Fig. 4.11, in case of single QW the results gradually declined from 0.69mA at the CL of 50μm to 0.11mA for the CL of 129μm. It remained same until 230μm. It further increased and ended at 0.15mA for CL of 339μm.

For the double QW the results started with 0.45mA and declined to 0.12mA for the CL of 149μm. After that it gradually increased and ended at 0.20mA for the CL of 339μm.

For the 5QW the results started with a lower value of 0.14mA for the CL of 50 μm then declined for the CL of till 80 μm and then it gradually increased to end at 0.37mA for the CL of 339μm.

Comparing these three scenarios this is observed that the best result is achieved for Single QW in terms of threshold current which is 0.11mA for the CL of 129μm and in terms of CL the best result is provided by the 5QW that provided threshold current 0.12 for the CL of 60μm.

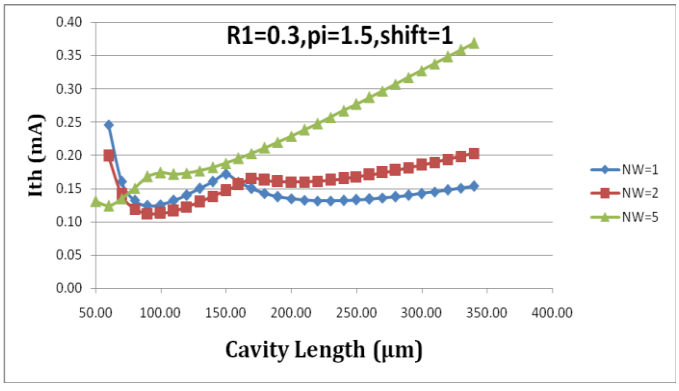

Fig. 4.12 Comparison among QWs forR1 = 0.3, π = 1.5, shift = 1

In Fig. 4.12, in case of single QW the results are quite fluctuating. It started from 0.25mA for the CL of 60μm and declined till CL of 109μm with the value of 0.13mA. After that, increased gradually up to 149μm with the value of 0.17mA current. Then, it declined to 0.13mA for the CL of 259 μm. Then it further increased and ended to 0.15mA for the CL of 339 μm.

For the double QW the results started with 0.20mA and declined to 0.11mA till the CL of 99μm. After that it gradually increased and ended at 0.20 for the CL of 339 μm.

For the 5QW the results started with a lower value of 0.13 for the CL of 50 μm then it gradually increased to end at 0.37 for the CL of 339 μm.

Comparing these three scenarios this is observed that the best result is achieved for Double QW both in terms of threshold current and CL, which is 0.11mA for the CL of 99 μm respectively.

5. Results

The conditions for the lowest threshold current could be summarized as following:

Facet reflectivity, R= 0.03,
Stripe width, w_s = 1.0 * 1.0e-6;
Number of active layers, n_w = 2;
Active thickness d_act = 6.5 * n_w * 1.0e-9;

FOR region 1: DFB
Wire width = 100 * 1.0e-9 nm
Pitch of grating = 240 * 1.0e-9 nm
Optical confinement factor: xi_m[1] = 0.02;
xi_s[1] = 0.00;
Loss: alpha_ac[1] = 100 *100;
alpha_ex[1] = 4 *100;

FOR region 2: DBR
Wire width = 70 * 1.0e-9 nm
Optical confinement factor: xi_m[2] = 0.02;
xi_s[2] = 0.00;
Cavity length of region2: 600 * 1e-6 μm

6. Conclusion

The research on photonic devices and photonic integration is going on all around the world to meet the high demand of data and telecommunication. In this study, an alternative but potential technology of quantum wire structure for photonic integration has been studied. For the current study we have mainly focused on studying a very low-threshold, high-efficiency and high speed modulation semiconductor laser using width-modulated structures.
The DR lasers, consisting of a DFB laser with high reflection DBR on one end, were realized by the formation of wire-like active regions for the DFB section. A low-threshold property was obtained. An ultra-low threshold current of 0.08mA can be obtained at a short cavity length of 100 μm for $\lambda/4$ shifted single QW DFB lasers with wire-like active regions. But single QW lasers have less output power, so there was a better option than it. Threshold current of 0.09mA can be obtained at a very short cavity length of 60 μm for $\lambda/4$ shifted double QW DFB lasers with wire-like active regions.

Reference

[1] Dr. H. Ghafouri–Shiraz, "Distributed Feedback Laser Diodes and Optical Tunable Filters" ,John Wiley & Sons Inc.,2003.

[2] Nobuhiro NUNOYA, "1.5-1.6 μm GaInAsP/InP Semiconductor Lasers with Fine Wirelike Active Regions ", Tokyo Institute of Technology.

[3] T. H. Maiman, R. H. Hoskins, I. J. D'Haenens, C. K. Asawa and V. Evtunov, "Stimulated optical emission in solids," *Phys. Rev*., vol. 123, no.4, pp. 1151-1157, Aug. 1961

[4] A. Javan, W. R. Bennet, Jr. and D. R. Herriot, "Population inversion and continuous optical maser oscillation in a gas discharge containing a He-Ne mixture," *Phys. Rev. Lett*., no. 6, p. 106, Feb. 1961.

[5] N. Holonyak, Jr. and S. F. Bevacqua, "Coherent (visible) light emission from Ga(As1-xPx) junctions," *Appl. Phys. Lett*., vol. 1, no. 4, p.82, Feb. 1962.

[6] J. -I. Shim, K. Komori, S. Arai, I. Arima, Y. Suematsu, and R. Somchai, "Lasing characteristics of 1.5 _m GaInAsP-InP SCH-BIG-DR lasers," *IEEE J. Quantum. Electron.*, vol. 27, pp. 1736-1745, June 1991.

[7] H. -C. Kim, H. Kanjo, S. Tamura, and S. Arai, "Narrow-stripe distributed reflector lasers with first-order vertical grating and distributed Bragg reflectors," *IEEE Photon. Technol. Lett.*, vol. 15, pp. 1032-1034, Aug. 2003.

[8] S. M. Ullah, "Monolithic Integration of Photonic Devices with Wirewidth Modulated Active Regions",Ph.D thesis, Tokyo Institute of Technology.